Performances in Case of Fire of Concrete Members Reinforced with FRP Rods: Experimental Results and Bond Models

E. Nigro [1], A. Bilotta [2], G. Cefarelli [3], G. Manfredi [4] and E. Cosenza [5]

ABSTRACT: Experimental tests were recently performed to evaluate the performances of nine concrete slabs reinforced with Fiber Reinforced Polymer (FRP) bars (continuous end to end) in fire situation by varying (a) external loads in the range of the service loads, (b) concrete cover in the range of usual values (30-50 mm), (c) bar end shape (straight or bent) and its length at the end of the concrete members, namely in the zone not directly exposed to fire (250-500 mm). Experimental results showed the importance of concrete cover in the zone directly exposed to fire for the protection provided to FRP bars, due to its low thermal conductivity. Moreover, the length of the FRP bars in the zone of slab not directly exposed to fire and its shape at the end of the members was crucial to ensures slab resistance once the resin softening reduced the adhesion at the FRP-concrete interface in the fire exposed zone of slab. In particular the anchorage obtained simply by bending bars at the end of member in a short zone (about 250 mm) allowed attaining a good structural behavior in case of fire equivalent to that showed by slabs characterized by a large anchoring length (about 500 mm). Tests results are briefly compared and discussed in this paper, whereas the behavior of the bar anchorage is carefully examined based on both the results of numerical thermal analysis and the predictions of a bond theoretical model adjusted for fire situation.

1 INTRODUCTION

Even if several international codes (CAN/CSAS806, ACI 440.1R-04, CNR-DT203/2006 are available for the design of concrete structures reinforced with Fiber Reinforced Polymer (FRP) bars, few provisions and calculation models taking account of fire situation are suggested. Consequently FRP-Reinforced Concrete employment is limited mainly to applications, where fire resistance aspects are not particularly meaningful. Hence, in order to improve the confidence in the use of FRP-RC members in multi-story buildings, parking garages, and industrial structures, the performances of these materials in fire situation must be evaluated. Experimental tests were recently performed by the authors to evaluate resistance and deformability of FRP-RC slabs (Nigro et al., 2011a,b,c). The experimental results are briefly mentioned in the first section of the paper and examined in the second section by a bond model taking into account the effects of temperature. In the third section design abaci, which allow the anchorage length of the bars in protected zones of the ordinary FRP-RC slabs to be assessed, are finally showed.

[1] *Associate Professor, Dept. of Structural Engineering, University of Naples "Federico II", emidio.nigro@unina.it*
[2] *PhD, Dept. of Structural Engineering, University of Naples "Federico II", antonio.bilotta@unina.it*
[3] *PhD, Dept. of Structural Engineering, University of Naples "Federico II", giuseppe.cefarelli@unina.it*
[4] *Full Professor, Dept. of Structural Engineering, University of Naples "Federico II", gamanfre@unina.it*
[5] *Full Professor, Dept. of Structural Engineering, University of Naples "Federico II", cosenza@unina.it*

2 EXPERIMENTAL PROGRAM AND RESULTS

The testing program (Nigro et al., 2011a,b,c) involved the design and fabrication of nine full-scale concrete slabs reinforced with GFRP bars, without fire protection system.
The main geometrical properties of all of the nine slabs divided into three sets (namely Set I: S1,S2,S3, Set II: S4,S5,S6 and Set III: S7,S8,S9) are showed in Table 1. The experimental investigation involved standard fire tests on simply-supported slabs. Three slabs (S1, S2 and S3) were 3500 mm long, 1250 mm wide and 180 mm thick; the concrete cover with reference to the bar centroid was 32 mm. The slabs S4, S5 and S6 were 4000 mm long, 1250 mm wide and 180 mm thick; the concrete cover was 51 mm. The slabs S7, S8 and S9 were identical to the slabs S1, S2 and S3, respectively, except for the shape of the longitudinal bottom bars bent at the end (see Figure 1). In order to avoid forming bar splice anchorages in the span of the slab, a single GFRP bar whose length was that of the slab minus 20 mm (i.e. twice the 10 mm of concrete cover at each end of the slab) was employed for every slab. The slabs were designed according to CNR-DT203. The design bending moment resistance of slabs was equal to $M_{Rd,1} \cong 65$ kNm except for the slabs S3, S6, S9 for which $M_{Rd,2} \cong 46$ kNm. Further details are reported in Nigro et al., 2011a,b,c.

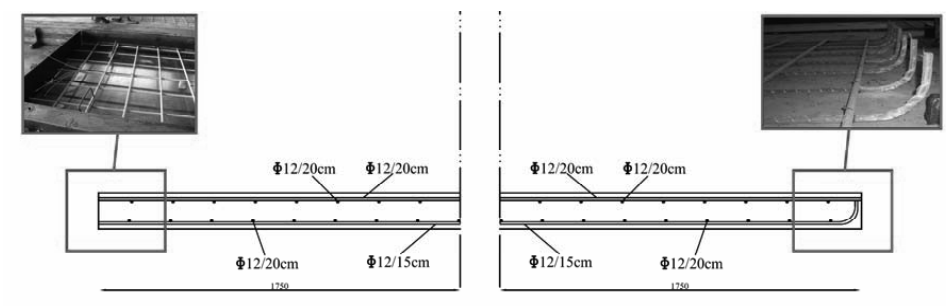

Figure 1 - Geometrical details of slabs S1,S2,S7,S8 (dimensions in millimeters) - Detail of bars' end.

Table 1 - Fire test main parameters for FRP reinforced concrete slabs.

Set	Slab	Length [mm]	Width [mm]	Thickness [mm]	Cover [mm]	Bottom bars (diameter/spacing) [mm]		Anchoring length [mm]	Bar shape
						longitudinal	transversal		
I	S1	3500	1250	180	32(*) 26(**)	Φ12/150	Φ12/200	250	Straight
	S2								
	S3					Φ12/225			
II	S4	4000	1250	180	51(*) 45(**)	Φ12/125	Φ12/200	500	Straight
	S5								
	S6					Φ12/200			
III	S7	3500	1250	180	32(*) 26(**)	Φ12/150	Φ12/200	250	Bent
	S8								
	S9					Φ12/225			

(*) thickness of concrete cover measured from the bottom concrete surface to the centre of bar
(**) distance from the bottom concrete surface to the nearest surface of reinforcement

2.1 Test set-up

The experimental investigation consisted of standard fire tests on the simply-supported slabs. Since the span between supports was 3200 mm, the slabs 3500 mm long (Set I and Set III) were external to furnace at each end for a length of 150 mm, whereas the slabs 4000 mm long (S4, S5, S6) for a length of 400 mm. A strip of about 100 mm of rock wool was used to protect the steel supports from fire exposure. Therefore, the ends of each slab were not directly exposed to fire action for a length, namely anchoring length, of about 250 mm for Sets I, III and 500 mm for Set II (Table 1). The slabs S1, S4, S7 have not loaded during the fire exposure. Slabs S2, S5, S8 and S3, S6, S9 have been loaded with a predefined service load corresponding to about the 40% and 60%, respectively, of the ultimate bearing capacity of the slab in normal temperature design. During the tests several the temperatures have been recorded along the FRP bars and within the concrete slab (Nigro et al., 2011a,b,c).

2.2 Main experimental remarks

The concrete cover was confirmed particularly meaningful for the protection provided to FRP bars, that allowing delaying the attainment of high temperature values in the bars. On the other hand, the experimental outcomes highlighted that, when in the directly exposed zone the bottom bar temperature exceed the glass transition temperature T_g, if a continuous reinforcement from side to side of the concrete element is used, the failure of the concrete slabs can be attained due to the rupture of the fibers in the middle of the member only if an adequate bar anchorage in the zones not directly exposed to fire is guaranteed. In the experimental program the anchorage was: (a) adequate when the length of the zone not directly exposed to fire was about 500 mm for straight bars or about 250 mm for bent bars, respectively, (b) inadequate when the length of the zone not directly exposed to fire was about 250 mm for straight bars. Further details regarding the fire tests of each slab are reported in Nigro et al., 2011a,b,c.

In the following section such experimental results related to the anchorage of the bars at the end of the members are analyzed by means of theoretical tools. At first, the stresses in FRP bars embedded in concrete slabs are estimated in fire situation through the incremental-iterative procedure proposed by Nigro et al., 2008. Moreover, a bond theoretical model calibrated in normal condition (Cosenza et al., 2002) and refined by authors in presence of high temperatures by using a model provided by Katz and Berman, 2000 is applied. The results are discussed in the following section with reference to the slabs reinforced with straight GFRP bars (set I and set II).

3 BOND MODELS AND DEVELOPMENT LENGTH

3.1 Assessment of FRP bars stresses

The strains, and therefore the stresses, in bars of slabs can be estimated by means an incremental-iterative procedure (Nigro et al., 2008), based on the hypothesis that plane-sections before bending remain plane after bending during all time of fire exposure.

Table 2 - Stresses in the anchorage of the bars at the end of the slabs S2, S3, S5, S6.

Slab	Exposure time [min]	Bending moment [kNm]	Failure type	Bar stress [N/mm^2]
S2	120	32.5	pull-out of bars	$\sigma'_{S2,120} \approx 250$
S3	60	27.6	pull-out of bars	$\sigma'_{S3,60} \approx 295$
S5	180	55.2	bars rupture	$\sigma'_{S5,180} \approx 305$
S6	180	46.0	bars rupture	$\sigma'_{S6,180} \approx 295$

As confirmed by experimental outcomes (Nigro et al., 2011a,b,c), already after about 30 minutes the temperatures recorded along the bottom bars during fire tests are noticeably

higher than T_g value, except for the bar ends in the zones of the slabs not directly exposed to fire. Thus, in fire exposed zone of slab the adhesion between FRP and concrete is negligible and the stresses, σ', can be considered constant along the bars. By contrast, in the zones of the slabs not directly exposed to fire the bond at FRP-to-concrete interface is possible due to low temperature. The stresses, σ', assessed according to the quoted incremental-iterative procedure for the slabs S2, S3, S5 and S6 at failure are listed in Table 2.

3.2 Assessment of the temperatures profile along the anchor length of the FRP bars

The readings provided by thermocouples in the zones not directly exposed to fire, both in same location of different slabs and in symmetrical locations of the same slab, resulted very scattered. This scattering is due to the experimental difficult on the assessment of both the exact location of thermocouples in the concrete slab and also the position of rock wool insulating ends of slabs in the furnace. Thus, the numerous experimental readings of temperature available for both sides of the slabs S4, S5 and S6 at distances equal to about 300 mm and 400 mm from the end of the slabs (Nigro et al., 2011a,b,c) were averaged. These mean values were assumed as the temperature at a distance of 350 mm from the end of the slabs, i.e. an average distance between 300 mm and 400 mm. The thermal field at the slab end was assessed by means of the nonlinear 3-D Finite Element software SAFIR2007 developed at the University of Liege and validated on the basis of experimental readings in the exposed area of the slab that were much less scattered (Nigro et al., 2011b). In the thermal model the extension of the unexposed zone was varied in order to match the simulated temperatures with experimental ones at 350 mm from the end of the slab. So, in the ends of slabs the thermal field during the tests could be better assessed. In Figure 2 and Figure 3 the temperatures evaluated along the bars anchor length at time of 180 min in slab S5 and 60 min in slab S3 are reported, respectively. The abscissa z = 0 mm is the section between fire exposed and unexposed zone.

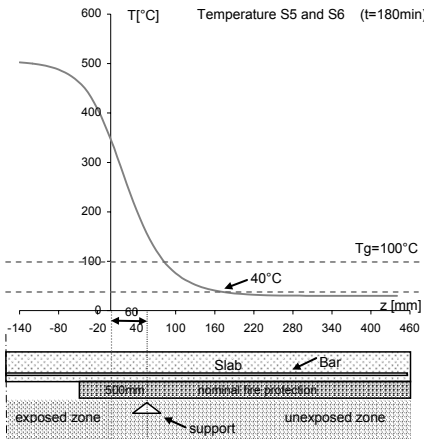

Figure 2 - Temperatures evaluate in the unexposed zones of Slabs S5 and S6 (t = 180 min).

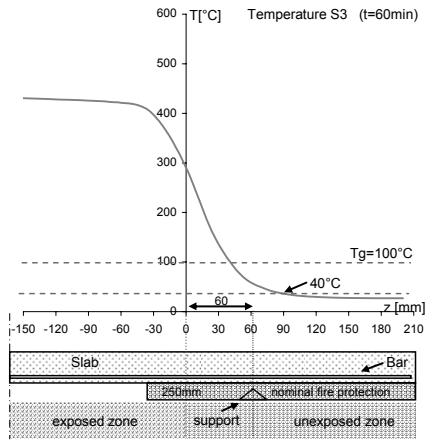

Figure 3 - Temperatures evaluate in the unexposed zones of Slab S3 (t = 60 min).

Note that experimental temperatures were better simulated by assuming 460 mm and 210 mm long unexposed zone. As stated above, such a value, slightly lower than nominal values (i.e. 500 mm and 250 mm), are justified by objective difficulties of ensuring perfect zone not directly exposed to fire due to both the type of protection used (mineral wool) and the accurate positioning of the slab on the furnace roof by mechanical equipment. On the other hand, the simulations which allowed the temperatures inside the slab to be evaluated were performed assuming the same thermal properties material and the same equations of heat transfer used for simulation reported in Nigro et al., 2011b: several comparisons

between simulation results and experimental readings showed the good reliability of the results of the analysis of thermal field. For this reason, for better interpreting the experimental data, the anchorage zone nominally not directly exposed to fire for a length of about 500 mm and 250 mm will be identified by the nominal length whereas the temperature profiles obtained by the numerical simulations will be referred to unexposed zones 460 mm and 210 mm long, respectively.

3.3 Assessment of FRP bars development length

Cosenza et al., 2002 identified a constitutive shear stress-slip law for FRP bars to concrete interface, constituted by:

- an ascending branch $$\tau_b(s) = \tau_m \cdot \left(\frac{s}{s_m}\right)^{\alpha} \quad \text{for slip } s \le s_m, \qquad (1)$$

and

- a softening branch $$\tau_b(s) = \tau_m \cdot \left(1 + p - p\frac{s}{s_m}\right) \quad \text{for slip } s > s_m, \qquad (2)$$

Therefore, the ''double branch'' constitutive law is completely defined when the values of τ_m, s_m, α, and p are predetermined. These parameters could be evaluated by means of an identification procedure minimizing the scatter between theoretical predictions and experimental results of pull-out tests. It was showed (Pecce et al., 2001) that reasonable variations of concrete strength influence not significantly the results, whereas more determinant is the typology of bar (material and surface treatment). Pecce et al., 2001 performed pull-out tests on sand coated GFRP bars quite similar (in terms of strength, stiffness and surface preparation) to those used to reinforce the slabs on which the fire tests were performed. Also the strength of concrete used for specimens of pull-out tests was quite similar to that of slabs. Mean values of parameters and corresponding coefficients of variation (*CV*) provided by Pecce et al., 2001 are:

s_m = 0.253 mm (0.181) τ_m = 14.65 MPa (0.110) α = 0.245 (0.619) p = 0.128 (0.599).

Note that the larger *CV* is relative to the parameter p, which represents the slope of the softening branch, and the parameter α, whereas τ_m and s_m values are less scattered. Moreover, through personal communication (Poggi and Carvelli, 2009), it was confirmed that pull-out tests performed on the same bars used in the slabs, and embedded in concrete specimens characterized by strength similar to that of the use to cast the slabs, provided an average maximum shear stress equal to 8.9 MPa. Therefore, in order to evaluate the development length of FRP bars at normal temperature condition, the following parameters were finally adopted in the model relationships (1) and (2):

$$s_m = 0.253 \text{ mm} \qquad \tau_m = 8.9 \text{ MPa} \qquad \alpha = 0.25 \qquad p = 0.128.$$

With reference to slabs S5 and S6, for the stresses $\sigma'_{S5,180} \approx 305$ N/mm^2 and $\sigma'_{S6,180} \approx 295$ N/mm^2 (see Table 2) the model provided a development length, $l_{d,S5} \approx 150$ mm and $l_{d,S6} \approx 145$ mm at room temperature (i.e. in the range of 20-40°C), respectively. On the other Figure 2 clearly shows that at 180 min the temperatures are lower than 40°C between z = 160 mm and 460 mm, namely for a length $l_{S5,40°,180} \approx 300$ mm larger than $l_{d,S5} \approx 150$ mm and $l_{d,S6} \approx 145$ mm. Thus, at this exposure time the anchorage length of the bars in fire unexposed concrete zone was clearly enough to avoid pull out of bars, as the experimental investigation showed (Nigro et al, 2011a). Furthermore ,when the load was increased, the slabs failed due to rupture in the fibers that achieved their tensile strength, which is clearly lower than experimentally evaluated at room temperature, due to the high temperature ($T_{S5,E,180} \approx 500$°C).
With reference to the slab S3, for the stress $\sigma'_{S3,60} \approx 295$ N/mm^2 (see Table 2), the model provided a development length, $l_d \approx 155$ mm at room temperature. On the other hand, the zone in which the temperatures could not influence the FRP to concrete bond

(lower than 40°C) were shorter (i.e. 140±10 mm considering 10 mm for the lateral concrete cover) as showed by temperature values of slab S3 reported in Figure 3.
In order to take into account the effect of high temperature on the bond of FRP reinforcing bars to concrete it was essential to consider the results provided by tests carried out by Katz et Berman (2000): indeed, their results indicate a severe reduction in the bond strength as the temperature at the surface of the rods rises up and goes over the T_g value. The expression for the normalized bond strength provided by Katz and Berman, 2000, taking into account the effect of the temperature, T, and the bar properties (i.e. normalized residual bond strength, τ_r^*, degree of cross linking, C_r, and glass transition temperature of the polymer at the surface of bar, T_g), is:

$$\tau^*(T) = 0.5\cdot\left(1-\tau_r^*\right)\cdot\tanh\left\{-\frac{0.02}{C_r}\left[T-\left(T_g+\frac{k_1}{0.02}C_r\right)\right]\right\}+0.5\cdot\left(1+\tau_r^*\right) \qquad (3)$$

The following parameters, related to the GFRP bars embedded in the slab, were adopted in the relationships (3):

$$\tau_r^* = 0.10 \qquad C_r = 90 \qquad T_g = 100\ °C.$$

The normalized residual bond strength, τ_r^*, was completely neglected for temperature higher than 250°C (Figure 4).

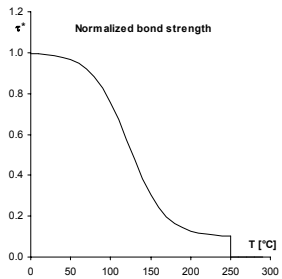

Figure 4 - Normalized bond strength vs. temperature.

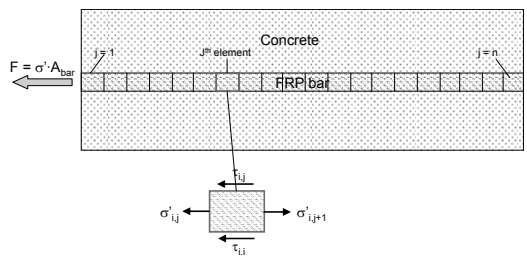

Figure 5 - Discretization of the FRP bars anchor.

The effect of the temperature on the shear stress-slip law expressed in Eq. (1) and Eq. (2) can be taken into account varying the parameter τ_m according to the Eq.
(3) by means of temperature curves *T(z)* plotted in Figure 2 and Figure 3, for the slabs S5, S6 at 180 min and the slab S3 at 60 min, respectively. Therefore the differential equation (4) that governs the bond problem of FRP bars is adjusted in:

$$\frac{d^2 s(z)}{dz^2} - \frac{4}{E(T(z))\phi}\tau^*\left(s(z),T(z)\right) = 0 \qquad (4)$$

where E and ϕ are the Young modulus and diameter of FRP bars respectively, and τ^* is a function of the bar temperature at the position z (Figure 2 and Figure 3) via Eq.
(3). Young's modulus dependence on temperature *E(T)* was also taken into account via the following reduction factor, calibrated by fitting the experimental data available in literature related to tensile tests performed on GFRP bars (Nigro et al., 2008):

$$\rho_E(T) = \frac{E(T)}{E} = \frac{0,28}{0,28+6,0\cdot10^{-12}\cdot T^{4,3}} \qquad (5)$$

where E is the Young modulus at normal temperature.
In order to solve Eq. (4) and, hence, to assess the development length of FRP bars, $l_{d,fi,t}$, in fire condition at time, t, an iterative finite differences procedure was used: it is briefly

described below. The FRP bar ends in the unexposed zone of the slab can be divided in "n" elements characterized by a length Δz = 1 mm (Figure 5) little enough to assume for each j^{th} element mean values of slip, $s_{i,j}$, and shear stress, $\tau_{i,j}$ (subscript "i" indicates the i^{th} iteration). One end of j = 1 part corresponding to z = 0 while one end of $j = n$ part corresponding to the end of slab (Figure 2 and Figure 3). Moreover, given $\sigma_{i,j}$ and $\sigma_{i,j+1}$ the normal stresses at the ends of j^{th} element (Figure 5) and $\Delta\sigma_{i,j}$ their difference, the following relationship can be written:

$$\sigma_{i,j+1} = \sigma_{i,j} - \Delta\sigma_{i,j} . \tag{6}$$

where $\Delta\sigma_{i,j} > 0$ is the bar normal stress transferred by shear stress to the concrete and it can be evaluated by equilibrium of the j^{th} element as:

$$\Delta\sigma_{i,j} = \tau_{i,j} \cdot (\pi \cdot \phi \cdot \Delta z) \ , \tag{7}$$

Finally the slip for the $j+1^{th}$ part can be evaluated as:

$$s_{i,j+1} = s_{i,j} - \left(\frac{\sigma_{i,j} + \sigma_{i,j+1}}{2 \cdot E} \right) \cdot \Delta z \ . \tag{8}$$

Therefore, given the stress in the first element (i.e. $\sigma_{1,1} = \sigma'_{S3,60} \approx 290$ N/mm^2 for the slab S3), once a tentative value of slip $s_{1,1}$ is assumed, the shear stresses $\tau_{1,j}$ and slips $s_{1,j}$ can be easily evaluated through Eqns. (1), (2) and Eq. (8), respectively, (varying j from 2 up to n). The procedure can be further iterated by varying the slip value $s_{i,1}$ until the value of j^* is determined satisfying the boundary conditions $s_{i,j^*} = 0$ and $\varepsilon_{i,j^*} = 0$ with a minimum tolerance of 10^{-5} with respect to $s_{i,1}$ and $\sigma_{i,1} = \sigma'_{S3,60}$, respectively. j^* is the part that delimits the development length. Being Δz = 1 mm, j^* value is the bar development length in fire condition, $l_{d,fi,t}$, in mm.

For the slab S3, at the fire exposure time of 60 min, the procedure provided a development length in fire situation $l_{d,fi,S3,60}$ = 189 mm very close to 200±10 mm available: such result agrees with the experimental result, i.e. the pullout of the bars at the end of the slab at 60 min. The values of normal stress, $\sigma'_{S2,120}$ = 250 MPa, and development length, $l_{d,fi,S2,120}$ = 193 mm, assessed for the slab S2 at experimental failure time (120 min), confirmed the results obtained on the slab S3.

For example, in

Figure 6 are plotted slips (a), shear stresses (b) and normal stresses (c) evaluated along the bar anchor related to slabs S3 at the experimental failure time, i.e. 60 min. The figure shows clearly the limit condition for the pull-out of the bar.

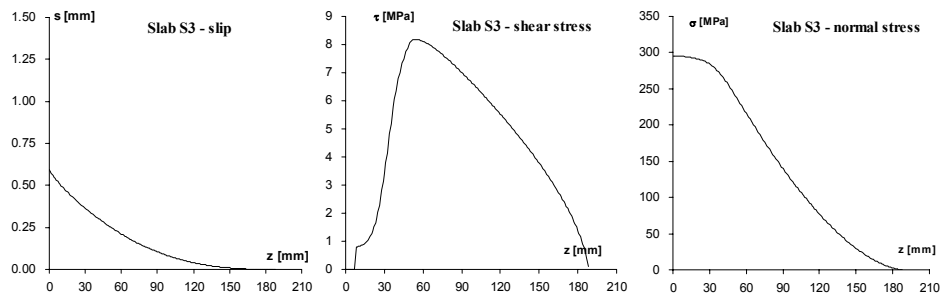

(a) (b) (c)

Figure 6 - Slips (a), shear stresses (b) and normal stresses (c) in the anchor of bars of slab S3 (t = 60 min)

At this point it seems clear that the bars slippage for the slabs of the set III characterized by cold zone equal to those of set I (i.e. about 250 mm) was prevented by the

construction detail (i.e. bar bent up to the top zone of the slab at its end) that allowed to achieve an effective anchorage, despite of short length of the cold zone. On the other hand, the theoretical predictions on the bond strength of the straight bars achieved a good agreement with the experimental results. Therefore, in the following section, design abaci allowing to asses the anchorage length in protected zones necessary for the reinforcement of ordinary FRP-RC slabs will be showed and discussed.

4 PARAMETRIC ANALYSIS AND DESIGN ABACI

Several thermal analyses were carried out on end zone of FRP-RC slabs characterized by a height h = 180 mm (i.e. the same height of the slabs experimentally tested) and a usual values of concrete cover (20 mm, 30 mm, 40 mm, 50 mm and 60 mm). The thermal input followed the ISO834 standard time-temperature curve. In Figure 7a are showed, for different time intervals corresponding to the classes of fire that are generally more common in the codes, the temperature profiles simulated to the centroid of the GFRP bars characterized by a concrete cover c = 20 mm. Similar temperature profiles were obtained for the other concrete cover value. The height of the slabs did not vary because for ordinary slabs (i.e. slabs characterized by a height ranging between 150 mm and 300 mm) the temperature is not particularly affected by this parameter, if also usual concrete cover (20 mm - 60 mm) are used. An extension of the area not exposed to fire, L_{unexp} = 250 mm, was defined on the safe side (the lower the value of L_{unexp} the higher the temperature, due to the lower capacity of the concrete to absorb heat). However, also this parameter does not particularly affect the values of the temperature. Because at 250 mm, for any value of concrete cover and fire exposure time, a temperature close to 20°C has always been calculated by the thermal simulations, it was possible to extend the results also beyond 250 mm by assuming a temperature constant of 20°C.

Through the Eqs. (1)-(8), introduced and discussed in the previous section to refine a bond theoretical model taking into account the effect of high temperatures, the theoretical anchorage length, L_b, in zone not directly exposed to fire necessary to transfer the forces between FRP bars and concrete were determined. Clearly, the parameters adopted in the model relationships (1) and (2):

$$s_m = 0.253 \text{ mm} \qquad \tau_m = 8.9 \text{ MPa} \qquad \alpha = 0.25 \qquad p = 0.128$$

are proper only for GFRP bars characterized by geometrical and mechanical properties similar to those considered so far.

In Figure 7b the values of L_b assessed for concrete cover, c = 20 mm, are plotted against the stress in the FRP bars (ranging between 100 MPa and 500 Mpa) for different times of fire exposure (ranging between 15 min and 180 min). Note that 500 Mpa is only the 50% of strength at normal condition of the bars used in the experimental program (i.e. 1000 MPa); nevertheless, it is quite close the GFRP design tensile strength, due to ordinary partial safety factor used for the design of FRP-RC members in normal situation (Ultimate Limit State – ULS). Therefore, in fire situation, the stress in the FRP bar must be lower than this value (Nigro et al., 2011a), due to design loads lower than those at ULS. The same curves are plotted in Figure 7c, Figure 7d, Figure 7e and Figure 7f for c = 30 mm, 40 mm, 50 mm and 60 mm, respectively.

The Figures 7b-f show that: (a) for c = 20 mm an anchor length, L_b, in zone not exposed to fire is always necessary also for low stresses (i.e. 100 MPa) and for small exposure times (i.e. 15-20 min); (b) also if a large concrete cover is adopted (e.g. c = 60 mm), an enough endurance of fire exposure (e.g. 60 min) can be guaranteed only if the bars are anchored in zones not exposed to fire for length higher as higher is the stress in the bar; (c) when the bar stress is 500 MPa, L_b ranges between 150 mm and 320 mm varying concrete cover and fire exposure time considered; (d) in any case, L_b never exceeds the value of about 320 mm even when the exposure time is equal to 180 min. Such results clearly depend on the properties of the FRP bars (i.e. fiber type, Young's modulus, tensile strength, diameter, surface treatment) and the strength of the concrete. The results can be extended to different types of bars as long as the manufacturer provides

the adhesion properties of the bars, at least under normal conditions. Note that an enough bond strength of the anchor can guarantee the fire resistance of FRP-RC member only if the bar stress is lower than its maximum tensile strength depending on its temperature. From this point of view, a high concrete cover value (i.e. 40-60 mm) can be more effective than a low concrete cover value (i.e. 20-30 mm).

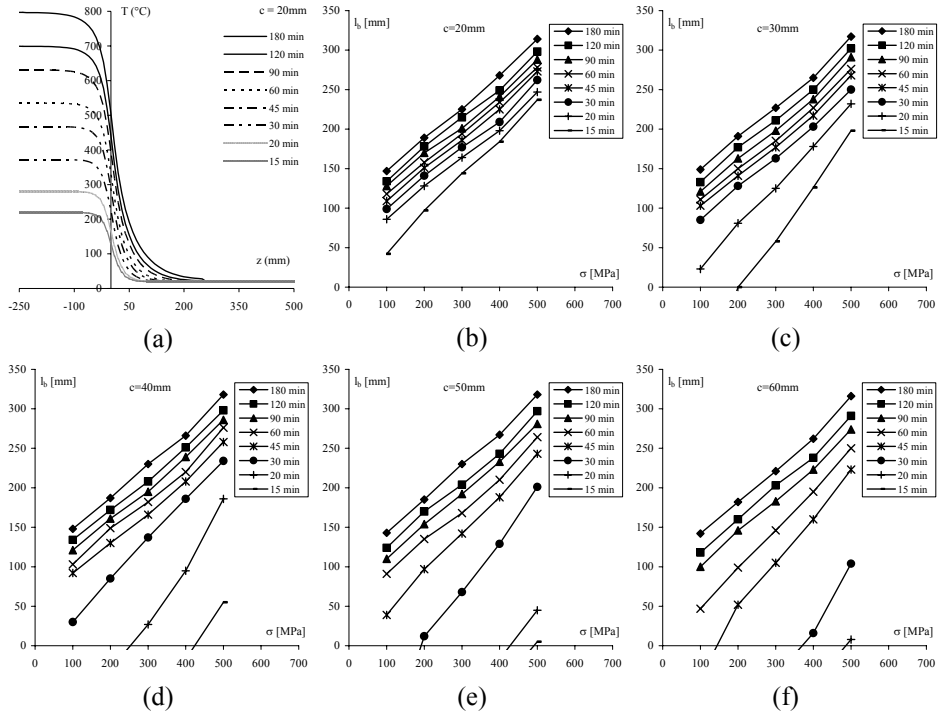

Figure 7 - Temperature in the anchorage zone (a) and anchorage length at different stresses for: (b) c = 20 mm, (c) c = 30 mm, (d) c = 40 mm, (e) c = 50 mm, (f) c = 60 mm.

5 CONCLUSIONS

Experimental results showed that the anchorage length of the FRP bars in the zone of slab not directly exposed to fire at the end of the members was crucial to ensures slab resistance once the resin softening reduced the adhesion at the FRP-concrete interface in the fire exposed zone of slab. In particular the anchorage obtained simply by bending bars at the end of member in a short zone (250 mm) allowed attaining a good structural behavior in case of fire, equivalent to that showed by slabs characterized by a large anchoring length (500 mm). Experimental results are briefly compared and discussed, whereas the behavior of the bar anchorage is examined based on the predictions of a bond theoretical model refined for fire situation. The theoretical predictions achieved a good agreement with the experimental results. Design abaci which allow to assess the anchorage length in protected zones necessary for the reinforcement of ordinary FRP-RC slabs have been obtained through the relationships of theoretical bond model taking into account the effect of high temperatures. For the specific FRP-RC members considered in the parametric analysis, it can be stated that:

- for low value of concrete cover, a minimum anchorage length, L_b, in zone not exposed to fire is always necessary, also if the bar stresses are low.
- the minimum anchorage length, L_b, never exceeds the value of about 320 mm even if the exposure time is equal to 180 min.

The results clearly depend on the properties of the FRP bars (i.e. fiber type, Young's modulus, tensile strength, diameter, surface treatment) and the strength of the concrete. However, they can be extended to different types of FRP bars as long as the manufacturer provides the adhesion properties of the bars, at least under normal conditions.

REFERENCES

ACI (2004), "*Guide for the Design and Construction of Concrete Reinforced with FRP Bars*" (ACI 440.1R-04), Farmington Hills, Michigan, USA.

CAN/CSAS806 (2002), "*Design and construction of building components with fiber reinforced polymers*".

CNR-DT203/2006, *Guide for the design and constructions of concrete structures reinforced with Fiber Reinforced Polymer bar*.

Cosenza E., Manfredi G., Realfonzo R.(2002), "Development length of FRP straight rebars", *Composites: Part B*, 33, 492-504.

EN1992-1-1, (2004) *Eurocode 2 -Design of concrete structures - Part 1-1: General rules and rules for building.*

EN1992-1-2, (2004) *Eurocode 2 -Design of concrete structures - Part 1-2: General rules - Structural fire design.*

Franssen J.M. (2007), "User's manual for SAFIR2007a, a computer program for analysis of structures subjected to fire", *University of Liege*, Belgium.

Katz A., Berman N. (2000), "Modeling the effect of high temperature on the bond of FRP reinforcing bars to concrete", *Cement & Concrete Composites,* 22, 433-443.

Nigro E., Cefarelli G., Bilotta A., Manfredi G., Cosenza E. (2011a), "Fire resistance of concrete slabs reinforced with FRP bars. Part I: experimental investigations on the mechanical behavior ". In press. *Composites: Part B*, doi:10.1016/j.compositesb.2011.02.025

Nigro E., Cefarelli G., Bilotta A., Manfredi G., Cosenza E. (2011b), "Fire resistance of concrete slabs reinforced with FRP bars. Part II: experimental results and numerical simulations on the thermal field". In press. *Composites: Part B* doi:10.1016/j.compositesb.2011.02.026

Nigro E., Cefarelli G., Bilotta A., Manfredi G., Cosenza E. (2011c), "Tests at high temperatures on concrete slabs reinforced with bent FRP bars", Proceedings of the 10th International Symposium on *Fiber Reinforced Polymer Reinforcement for Concrete Structures,* ACI SP-275, Farmington Hills, Michigan, USA.

Nigro. E., Manfredi G., Cosenza E., Cefarelli G. (2008), "High-temperature behaviour of concrete slabs reinforced with FRP bars", *Proceedings of CICE2008,* Zurich, Switzerland.

Pecce M., Manfredi G., Realfonzo R., Cosenza E. (2001), "Experimental and analytical evaluation of bond properties of GFRP", *Journal of Materials in Civil Engineering*, 13(4), 282-290.

Poggi C., Carvelli V. (2009), *Personal communication*. University of Milan. Italy.